ONLINE FIRST

This is a provisional PDF only. Copyedited and fully formatted versión will be made available at final publication

HISTOLOGY AND HISTOPATHOLOGY

ISSN: 0213-3911
e-ISSN: 1699-5848

Histological and stereological insights into renal and adrenal changes in pregnant rats exposed to wood smoke-derived PM2.5

Authors: P. Salinas, F. Villarroel, C. González-Torres, T. Lazcano, J. Silva, A. Maulen and E. Rojas

DOI: 10.14670/HH-18-863
Article type: ORIGINAL ARTICLE
Accepted: 2024-12-23
Epub ahead of print: 2024-12-23

Histological and stereological insights into renal and adrenal changes in pregnant rats exposed to wood smoke-derived PM2.5

P. Salinas[1], F. Villarroel[1-2], C. González-Torres[1], T. Lazcano[1], J. Silva[1], A. Maulen[3], E. Rojas[3]

[1] Laboratory of Animal & Experimental Morphology, Institute of Biology, Faculty of Sciences, Pontificia Universidad Católica de Valparaíso, Valparaíso, Chile

[2] MSc. Program in Biological Sciences, Pontificia Universidad Católica de Valparaíso, Valparaíso, Chile.

[3] Morphohistology Unit, School of Sciences, Universidad de Viña del Mar, Chile.

Short title: Renal and adrenal effects of wood smoke PM2.5 in pregnancy

Keywords: kidney, histology, stereology, wood smoke, PM2.5

Corresponding author:

Paulo Salinas

paulo.salinas@pucv.cl

ABSTRACT

Air pollution, particularly fine particulate matter (PM2.5), is a global health issue affecting millions. In southern Chile, firewood used for heating exacerbates pollution, especially in winter. This study examines the impact of wood smoke-derived PM2.5 on kidney and adrenal gland morphology in pregnant rats. It evaluates chronic PM2.5 exposure effects during pregestational and gestational periods in Sprague-Dawley rats. Pregnant rats were exposed to PM2.5 in Temuco, a city with high wood smoke pollution. Filtered and unfiltered air chambers simulated different exposure conditions. Histological and stereological analyses were conducted on rat kidneys and adrenal glands using systematic sampling and STEPanizer software. Findings showed significant changes in renal and adrenal morphology due to PM2.5 exposure. In the kidney, variations were observed in glomerular compaction, proximal convoluted tubules, and medullary rays. In the adrenal gland, the zona fasciculata showed decreased acidophilia and lipid content, reduced cytoplasmic homogeneity, and the appearance of empty spaces. These effects were more pronounced in rats exposed to unfiltered air during both pregestational and gestational periods. Wood smoke-derived PM2.5 exposure significantly impacts kidney and adrenal morphology in pregnant rats, emphasizing the need for strategies to reduce environmental pollutant exposure during critical developmental periods to protect maternal-fetal health.

INTRODUCTION

Air pollution is a global public health issue, affecting 92% of the world's population living in areas where the air quality exceeds the limits recommended by international guidelines (WHO, 2022). This problem is associated with approximately 4.3 million deaths due to indoor air pollution and 3.7 million due to outdoor air pollution annually. Atmospheric pollutants, particularly particulate matter (PM2.5; aerodynamic diameter ≤ 2.5 micrometers), are of particular concern due to their ability to penetrate the respiratory system and disperse throughout the body via the bloodstream, posing a significant health risk.

Exposure to air pollution during pregnancy adversely affects placental and fetal development (Salinas et al., 2020; Villarroel et al., 2024), leading to intrauterine growth restriction, prematurity, low birth weight, congenital anomalies, and in extreme cases, intrauterine and perinatal death. It also compromises endometrial functionality by affecting critical parameters for embryonic implantation, such as uterine morphological differentiation (de Castro et al., 2024) and maternal respiratory function, impacting oxygen and nutrient supply to the fetus via the placenta (Zhu et al., 2021). High concentrations of PM2.5 have been linked to placental inflammation, abnormalities in trophoblastic invasion, and reduced placental angiogenesis, adversely affecting fetal development (Santos et al., 2021). During pregnancy, the kidneys play a crucial role in regulating the glomerular filtration rate (GFR), electrolyte management, and acid-base balance (Beers and Patel, 2020; Alsuwaida et al., 2011). Pregnancy induces systemic vasodilation, increasing renal blood flow and GFR by 50 to 60% (Beers and Patel, 2020). Additionally, increased creatinine clearance is observed due to these changes in renal function. Although adrenal gland disorders are rare during pregnancy, their deficiencies or excesses can trigger both fetal and maternal morbidity. Pregnancy demands increased steroid production to support fetal growth and meet maternal needs, leading to a physiological state of hypercortisolism. This period is characterized by elevated levels of adrenocorticotropic hormone (ACTH), cortisol, aldosterone, deoxycorticosterone, and corticosteroid-binding globulin (CBG), without a significant increase in adrenal gland weight, despite the expansion of the zona fasciculata, the primary producer of glucocorticoids (Levin et al., 2019).

Proper adrenal gland and kidney functionality during pregnancy is crucial for maternal health and fetal development (Afsar et al., 2019). Compromises in these organs can negatively impact fetal development. Prenatal and gestational exposure to PM2.5, especially from wood smoke, raises significant concern due to its potential to alter kidney and adrenal gland structure and function. Existing studies have established a direct relationship between prenatal exposure to PM2.5 from industrial and traffic sources and adverse effects in pregnant women, such as reduced birth weight and impaired renal function (Xie et al., 2022). Additionally, exposure to PM2.5 has been shown to reduce the GFR and increase blood urea nitrogen and uric acid levels, implying an increased risk of kidney disease (Mehta et al., 2016). PM2.5 exposure also induces oxidative stress and inflammatory responses, with increased production of reactive oxygen species (ROS) leading to renal damage and altered renal function. While most studies focus on non-pregnant populations, it is plausible that

gestational PM2.5 exposure could have similar or exacerbated effects due to physiological changes during pregnancy (Zhong et al., 2019).

PM2.5 exposure has been linked to alterations in endocrine function, including adrenal gland activity. Contaminants in PM2.5 can act as endocrine disruptors, interfering with the synthesis and metabolism of steroid hormones, including cortisol, a hormone produced by the adrenal gland. This could have significant implications during pregnancy as cortisol plays a crucial role in regulating metabolic processes, stress response, and fetal development (Liu et al., 2017). Any alteration in maternal renal or adrenal function could have direct consequences on fetal development. For example, alterations in water and electrolyte balance regulation due to renal dysfunction can affect the uterine environment, while changes in adrenal hormone production can influence fetal maturation and timing of delivery (Thompson and Al-Hasan, 2012). Understanding these effects is critical for developing mitigation and protection strategies for this vulnerable population.

Given the potential of PM2.5 to adversely affect both renal function and adrenal gland activity during pregnancy, this study aims to investigate how prenatal and gestational exposure to PM2.5, originating from wood smoke used for heating, affects the morphology of the kidney and adrenal gland in pregnant females. We hypothesize that prolonged exposure to PM2.5 causes significant structural changes in these vital organs of pregnant rats, suggesting that such exposure could alter organ proportion and structure due to PM2.5 pollution. The study aims to evaluate the effects of chronic PM2.5 exposure from wood smoke, specifically during the pregestational and gestational periods, on the structure of the kidney and adrenal gland. The goal is to obtain information on the implications of this specific form of environmental pollutant on pregnancy and fetal development.

2. MATERIAL Y METHODS

2.1 Exposure location and animals

Pregnant Sprague-Dawley rats belonging to the university bioterium were utilized in the city of Temuco, located in southern Chile (38°44'59.4"S 72°37'07.8"W). The selection of this location was based on its designation as one of Chile's most polluted cities, according to IQAir (2019, 2022). Additionally, residential use of wood stoves has been reported as its primary source of air pollution (Blanco et al., 2022). The association between exposure to wood smoke-derived air pollution and maternal renal and adrenal stereological parameters was investigated using a time-stratified crossover design. All procedures were conducted in accordance with Law 20.380 (Ministry of Agriculture, 2009) and were approved by the Scientific Ethics Committees of the University of La Frontera (Act 122/20) and the Bioethics and Biosafety Committee of the Pontificia Universidad Católica de Valparaíso (Act BIO EPUCV-BA 373-2020). Two generations of rats were exposed to air pollution primarily from wood smoke combustion, and the second generation (G2) was used to investigate the effects of prenatal exposure from previous generations.

2.2 Exposure conditions

The exposure was carried out by simulating two adjacent environments, as described by Veras et al. (2008), aiming to generate a gradient in PM2.5 levels through the filtration of ambient air, conducted in an urban area with a history of air pollution and in proximity to the air quality monitoring station. Two open chambers were utilized, following the description by Villarroel et al. (2024), both receiving ambient air at a flow rate of 20 m^3/min and maintained under similar environmental conditions in terms of temperature and humidity. Each chamber was 2.1 m x 2.0 m x 2.1 m, with the capacity to accommodate up to 50 animal cages. Air entered the chambers through a fan located at the base, with a flow rate of 150 m^3/h, distributed uniformly before being expelled through a wide opening at the top. The system remained normobaric, with the internal pressure of the chambers not exceeding 40-60 mmH_2O. Air was filtered in only one of the chambers, using three filters in series. The first two filters, metallic and pleated, were responsible for retaining large and medium-sized particles, while the third consisted of a Purafil PSA 102 gas filtration unit (Purafil, Inc., U.S.A) equipped with Purafil Select filter media in PK12 modules (Purafil, Inc., U.S.A) (Fig. 1A-B).

2.3 Experimental design and groups

Two generations of rats were exposed to air pollution from wood smoke, focusing on the second generation (G2) to investigate the effects of prenatal and gestational exposure based on Veras et al. (2008). G2 rats were obtained using the following protocol (Fig. 1C): 20-day-old G0 rats (10 males and 10 females) were housed in filtered air (FA: 5 pairs) and non-filtered air (NFA: 5 pairs) chambers. G0 rats mated within their respective chambers upon reaching reproductive maturity, around 60 days of age. The resulting G1 offspring remained in the same environment. G2 rats were then produced from the mating of 10 pairs of G1 rats (FA: 5 pairs; NFA: 5 pairs). During the pregestational period, G2 rats were continuously exposed to filtered air (FA; n=48) or non-filtered air (NFA; n=48) until mating. Subsequently, during the gestational period, fertilized G2 females were divided into four study groups until delivery: FA/FA (control, n=12; G2 females raised and gestated in filtered air), FA/NFA (n=12; females raised in filtered air and gestated in non-filtered air), NFA/FA (n=12; females raised in non-filtered air and gestated in filtered air), and NFA/NFA (n=12; females raised and gestated in non-filtered air). The primary outcome measure for determining sample size was the morphological changes in the kidney and adrenal gland, specifically alterations in glomeruli density (Nv [Glo/μm^2]) and spongy cortical endocrinocyte volume density (Vv [%] SCE) in the zona fasciculata. Sample size calculations were based on expected differences between the control (FA/FA) and PM2.5 exposed groups (NFA/NFA), using prior similar studies to estimate effect size and variability, ensuring sufficient power to detect significant differences.

2.4 Kidney and adrenal gland collection

A surgical procedure was developed in three phases: preoperative, surgical, and postoperative. During the preoperative phase, the rat's abdominal area was prepared, including shaving and disinfecting with a 2% chlorhexidine solution, followed by 70% alcohol to remove surface fats. This stage was completed by placing

sterile surgical drapes designed with a surgical window to facilitate access to the incision site. The surgical phase involved performing a laparotomy and cesarean section on day 20 post-fertilization, coinciding with the standard gestational period for Sprague Dawley rats. To ensure animal welfare during these procedures, a combination of ketamine/xylazine was administered at doses of 80 mg/kg and 10 mg/kg IP, respectively, as a sedation/anesthesia protocol. From each group of rats, a kidney and the adrenal gland were extracted for analysis, ensuring careful handling to avoid compromising the adrenal gland's integrity. This process was facilitated using blunt forceps to grasp the perirenal adipose tissue, allowing for the gentle extraction of the kidney. The obtained organs were subsequently cleaned, dissected, and fixed in 5% formalin for further analysis, following the protocols established by Van Koppen et al. (2013), thus ensuring procedural standardization and the reliability of the obtained results. The postoperative phase was critical for the animals' recovery, during which analgesics and antibiotic therapy were administered.

2.5 Renal volumetry

The Scherle method was used to determine the renal volume (Nyengaard, 1999). First, a beaker filled with physiological saline solution was prepared and placed on a precision balance. Immediately after surgical removal, the kidneys were then carefully suspended inside the beaker using a fine thread, ensuring that the organ did not touch the walls or the bottom of the container, thereby guaranteeing an accurate measurement of the liquid displacement. This procedure was repeated twice for each kidney from the different study groups to ensure the reliability and reproducibility of the obtained data.

2.6 Tissue Preparation

To adjust the methodology and account for variations in the shrinkage artifact of kidney tissue, we calibrated the microtome block advance by measuring the change in block height divided by the number of sections cut, ensuring an accurate estimate of the average section thickness (Gundersen et al., 1988; Dorph-Petersen et al., 2001; Tschanz et al., 2011). Additionally, we used a systematic uniform random sampling method to measure section thickness at different positions, employing a micrometer to record the vertical movements of the microscope stage. This methodology allowed us to adjust volumetric density calculations and other morphometric measurements to correct for any bias introduced by differential section shrinkage. Finally, we employed oil immersion objectives to minimize optical biases and ensure accurate distance measurements along the z-axis. These methodological adjustments ensured that stereological estimates were unbiased, even in the presence of tissue shrinkage. To address variations in tissue contraction artifacts (Tschanz et al., 2011), we applied the methodologies described by Dorph-Petersen et al. (2001). To estimate the contraction index, a thin circular section was extracted from a random slice of the kidney and adrenal gland using a punch and needle, respectively, ensuring that its thickness was less than one-tenth of the average height of the particle to avoid overestimation. Also, we calculated volume deformation by comparing the sum of block volumes before and after embedding, allowing us to adjust for any volumetric changes during the processing stages. Subsequently, we estimated area deformation (AD) by comparing the section areas of the blocks before and

after sectioning, helping to account for any changes in tissue dimensions due to cutting. Additionally, we measured the local section thickness for each counting frame. These data were used to weight the calculations, ensuring that variations in shrinkage were accurately reflected in the final estimates. This approach ensured that, even with differential shrinkage among specimens, the calculations remained unbiased. By implementing these methods, we ensured that our stereological estimates were robust against variations in shrinkage artifacts, allowing us to combine data from different samples accurately and provide reliable averages and standard deviations. Following fixation, the samples underwent dehydration through a graded alcohol series, were cleared in xylene, and embedded in Paraplast (Paraplast Plus embedding medium; melting point: 54ºC; Sigma-Aldrich Chemical Co., St. Louis, MO, USA). Sections of 5 µm thickness were prepared using a Leica RM2255 motorized rotary microtome (Leica Microsystems, Switzerland). The sections were then rehydrated, treated with xylene for 10 minutes, and gradually hydrated through descending ethanol concentrations (100%, 96%, 80%, and 70%, each for 15 seconds), culminating in distilled water. Histological cross-sections of the kidneys were routinely stained with hematoxylin and eosin and imaged with a Motic Easy Scan Pro® digital slide scanner (Motic Instrument Inc, Canada) to generate comprehensive panoramic views. Throughout the histological processing, the generated cutting plane was maintained, serving as the plane for the histological sections. Given that the study was both descriptive and quantitative, hematoxylin-eosin staining was solely employed as it facilitated the analysis of digital images and the extraction of numerical data.

2.7 Histological study

A comprehensive histological analysis was conducted on the kidney and adrenal gland. In the kidney, variables such as the morphology of the proximal convoluted tubule (PCT), the structure of the medullary ray, the morphological characteristics of the glomeruli, the arterioles, and the thin segment of the nephron loop (*ansa nephronis; Loop of Henle*) were examined. In the adrenal gland, the variables included the cortex, the medulla, the zona fasciculata (ZF; *fasciculata zone*), the spongy cortical endocrinocytes (SCE, *endocrinocytus corticalis spongiosus*) of the ZF, the cortical blood vessels, and the drainage of the blood vessels and medullary chromaffin cells (MCC, *endocrinocytus medullaris*). All terms used in this study were according to the *Nomina Histologica Veterinaria* (International Committee on Veterinary Histological Nomenclature, 2017).

2.8 Sampling strategy

In this study, a systematic and uniformly random sampling approach was implemented to analyze the structure of both the kidney and adrenal gland, thereby optimizing the precision and efficiency of stereological sampling. One of the first n slices was randomly selected, and from there, every *n*-th slice was chosen for analysis. This method ensured that all slices had an equal probability of being selected, however, unlike random sampling, it established a fixed pattern that helped reduce sampling variance and improve the study's efficiency. This type of sampling was useful for obtaining a representative sample of the tissue with less variability and is preferable when studying structural characteristics that are uniformly distributed throughout the tissue, providing a robust framework for the detailed stereological analysis of the kidneys and adrenal gland.

2.9 Orientation of section planes

Given that the specific orientation of the structures of interest does not affect the estimation of the parameters, sections were cut without a predetermined orientation relative to the organ's structure. This orientation was sufficient for estimating parameters that do not depend on the orientation of the structures, such as the number of structures (*e.g.*, the number of glomeruli) and total volume using point counting. Arbitrary orientation is useful for general studies where the specific orientation of structures does not impact the estimation of the parameters of interest.

2.10 Image acquisition and stereological estimators

Images were captured using a Leica® DM750 optical microscope equipped with a Leica® MC170HD digital camera. The images were analyzed using the STEPanizer Stereological Tool software (Figure 2), applying the M36 point grid system (Tschanz et al., 2011). The stereological parameters evaluated in both the kidney and adrenal gland are detailed in Tables 1 and 2.

2.11 Statistical analysis

Data were organized in Excel 2021 tables (version 18.0 for Windows, Microsoft Office, 2021) and expressed as means and standard deviations. To determine data distribution, the Kolmogorov-Smirnov and Shapiro-Wilk normality tests were performed. Data were transformed to fit a normal distribution where necessary. To identify differences between groups, a one-way ANOVA and Tukey's *post-hoc* multiple comparison test were conducted. All tests were performed with a 95% confidence interval and a p-value of <0.05. Data were analyzed using Prism version 9.0 for Windows (GraphPad Software, San Diego, CA).

Table 1. Definition of stereological estimators in the kidneys of female Sprague Dawley rats exposed to PM2.5

Variable	Definition
Volume (ml)	Total volume of the kidney: total kidney volume for each group.
Vv (%) Glo	Glomerular volume density in the kidney cortex: proportion (%) of glomeruli present in a surface area of the studied renal cortex.
Vv (%) Glo/kidney	Glomerular volume density (%) in the kidney: proportion (%) of glomeruli present per surface area in the kidney.
Sv Glo ($\mu m^2/\mu m^3$)	Glomerular surface density per unit volume: surface area (μm^2) of a glomerulus per unit volume (μm^3) of the renal cortex.
Sv Glo/kidney	Glomerular surface density in total kidney volumes: surface area (μm^2) of a glomerulus in the total kidney volumes.
Nv (Glo/μm^2)	Number density of glomeruli in the kidney cortex: number of glomeruli in a given area of the kidney cortex (μm^2).

Vv (%) Cortex	Volume density of the cortex (%): proportion (%) of the cortex present per surface area in the renal parenchyma.
Vv (%) Medulla	Volume density of the medulla (%): proportion (%) of medulla present per surface area in the renal parenchyma.

Table 2. Definition of stereological estimators in the adrenal glands of female Sprague Dawley rats exposed to PM2.5

Variable	Definition
Vv (%) cortex	Volume density of the cortex (%) in the adrenal gland: proportion (%) of cortex present per surface area in the adrenal gland.
Vv (%) medulla	Volume density of the medulla (%) in the adrenal gland: proportion (%) of medulla present per surface area in the adrenal gland.
Vv (%) SCE	Volume density of SCE (%) in the zona fasciculata: proportion (%) of SCE present per surface area of the zona fasciculata.
Sv SCE ($\mu m^2/\mu m^3$)	Surface density of SCE in the zona fasciculata: surface area (μm^2) of SCE in the zona fasciculata.
Nv ($SCE/\mu m^2$)	Number density of SCE in the zona fasciculata: number of SCE in a given area (μm^2) of the zona fasciculata.

SCE: spongy cortical endocrinocyte

3. RESULTS

3.1 Renal histology

Variations in glomerular morphology were observed among different groups. The FA/FA group exhibited spherical and compact glomeruli with normal histological characteristics, including visible basophilic cell nuclei, acidophilic cytoplasm, and limited urinary spaces mainly between the layers of the glomerular capsule (*capsula glomeruli*) (Figure 3). In contrast, the NFA/NFA group showed sectioned glomeruli with subdivisions compromising their compactness and exhibited dilated urinary spaces. The FA/NFA group displayed more compact glomeruli than the NFA/NFA group, with reduced subdivision of urinary spaces, although with intermediate compactness and urinary space visualization compared with the FA/FA group. Finally, the NFA/FA group revealed a lower degree of glomerular compactness than the FA/NFA group and smaller urinary spaces compared with the NFA/NFA group, with no notable changes in the basophilic and acidophilic conditions of nuclei and cytoplasm between the groups.

In the study of PCT (*tubulus proximalis pars convoluta*) morphology among different experimental groups, significant variations were observed. The FA/FA group exhibited classic PCT morphology, characterized by

evident acidophilia with H-E staining, narrow lumens, and a distinctive brush border on epithelial cells, whose nuclei tended to shift from the central cellular zone, likely related to the tissue section orientation (Figure 3). Conversely, the NFA/NFA group showed areas where the PCT lost its typical structure, with anastomosed cells making it difficult to distinguish between cell shapes, lumen, and brush borders; however, preservation of typical morphology in certain areas suggests that these variations are due to experimental conditions and not technical artifacts. In contrast, the PCT in the FA/NFA group resembled that of the FA/FA group, with clearly identifiable cell structures, lumens, and brush borders, and no evidence of the cellular anastomosis observed in the NFA/NFA group. Finally, the NFA/FA group presented morphological changes in the PCT similar to those in the NFA/NFA group, but to a lesser extent, differentiating from the FA/FA and FA/NFA groups that did not show these variations.

The morphology of the medullary ray (*radius medullaris*) in different experimental groups revealed significant variations in the organization and structure of this renal component. In the FA/FA group, the medullary rays showed an organized structure, with clearly visible straight portions of tubules and minor collectors in longitudinal sections, extending from the medullary zone to the cortex and almost reaching the renal capsule (Fig. 3). In contrast, the NFA/NFA group presented an irregular arrangement of the medullary rays through the cortex, without evidence of a complete pathway to the renal capsule. The FA/NFA group, although showing superior organization compared with the NFA/NFA group, exhibited discontinuity in approaching the renal capsule, disorganizing in the last third of the cortex and manifesting a less evident medullary ray arrangement than in the FA/FA group. The NFA/FA group was marked by significant disorganization in the course of the medullary rays through the renal cortex, with difficult distinction of constituent tubules under light microscopy, which also altered the spatial distribution of the cortical labyrinth (*labyrinthus corticis*), clearly differing from the other study groups. In this study, arterioles located in the cortical labyrinth were examined, highlighting their large muscular tunica and the presence of an internal elastic membrane in their intima. The studied groups, following the order FA/FA, FA/NFA, NFA/FA, and NFA/NFA, showed a progressive increase in arteriole diameter based on the measurement of the internal elastic membrane. This observation suggests significant differences in arteriole caliber among the groups, although the structural components of the arteriole walls remained consistent without apparent morphological variations. The thin portion of the nephron loop (*ansa nephronis*) corresponds to an extension of the PCT that generally functions to control the osmolality levels of the ultrafiltrate. In the studied groups, it was observed to be composed of a simple squamous epithelium of variable height depending on whether it corresponds to cortical or juxtamedullary nephrons, as well as their total length. In general, no comparable significant differences in histological organization were observed among groups (Table 3).

3.2 Adrenal gland histology

The zona fasciculata, the most developed part of the adrenal cortex, accounting for 80% of the total cortical volume, was composed of large, polyhedral SCE arranged in long, straight cords. The cell cytoplasm exhibited

acidophilia due to the abundant presence of lipid inclusions, visible as small vesicles, resulting in a homogeneous cytoplasm. In the FA/FA group, the SCE showed characteristic lipid content and acidophilia, with cellular organization consistent with the literature and homogeneous cytoplasmic content, though with some retraction. In the NFA/NFA group, SCE exhibited reduced acidophilia and decreased lipid content, with no alterations in cellular organization but a noticeable decrease in cytoplasmic homogeneity, creating empty spaces. The FA/NFA group showed intermediate characteristics regarding lipid content, acidophilia, and cytoplasmic homogeneity between the FA/FA and NFA/NFA groups, with no alterations in cellular organization. Finally, the NFA/FA group presented cells with irregular lipid content, lower acidophilia, and less cytoplasmic homogeneity compared with the NFA/NFA group, although cellular organization remained unchanged. In the cortical blood vessels in the adrenal gland, fenestrated sinusoidal capillaries were observed, formed by endothelium with cytoplasmic spaces and discontinuities in their basal membranes, corresponding to the zona fasciculata. In the FA/FA group, the capillaries had compressed endothelial cell nuclei by the cellular cords characteristic of the zona, with a poorly visible or dilated lumen. In the NFA/NFA group, the capillaries showed non-compressed endothelial nuclei and a visible, dilated lumen compared with the FA/FA group. The FA/NFA group exhibited capillaries with endothelial nuclei and a lumen in a phase intermediate to the FA/FA and NFA/NFA groups, with visible blood content (erythrocytes). In the blood vessel drainage into the medullary sinuses of the adrenal gland (*plexus venosus medullae*), a dual circulation was observed in the medulla: one from the cortical arteriole, branching into fenestrated sinusoidal capillaries traversing the entire cortex and draining into the medullary sinuses, and another from the medullary arteriole, also draining into the venous sinuses and converging into the central medullary vein. In the FA/FA group, the fenestrated sinusoidal capillaries showed preserved walls and lumens with blood content, with visible drainage into the medullary sinuses. In the NFA/NFA group, fenestrated sinusoidal capillaries draining into the medullary sinuses were not observed. The FA/NFA group exhibited capillaries with preserved walls and lumens with blood content, though with less drainage into the medullary sinuses compared with the FA/FA group. Finally, the NFA/FA group displayed capillaries with similar characteristics but even less drainage into the medullary sinuses compared with the FA/NFA group. In the medulla, MCC nuclei were organized into ovoid groups and short anastomosed cords, showing different degrees of acidophilia and basophilia associated with their vesicular cytoplasmic components and function. In the FA/FA group, MCCs exhibited conserved nuclei with varying degrees of basophilia, with smaller nuclear sizes compared with the FA/NFA and NFA/FA groups. The NFA/NFA group showed MCCs with conserved nuclei and various degrees of basophilia, with nuclear sizes smaller than those in the FA/NFA, NFA/FA, and FA/FA groups. In the FA/NFA group, MCC nuclei were conserved and showed different degrees of basophilia, with a larger size compared with the NFA/FA group. Finally, the NFA/FA group displayed MCCs with conserved nuclei and varied degrees of basophilia, with a nuclear size intermediate to the FA/NFA group (Table 3).

3.3 Stereology

The results presented in Table 4 indicate significant differences in renal morphometry and stereology among the studied groups, highlighting variables such as the proportion of medullary volume (p=0.0131) and cortical volume (p<0.0001) in the kidney, as well as glomerular surfaces (p=0.0474). Table 5 reveals notable differences in the stereology of the adrenal gland, including the proportion of volume and surface area in the cortex and medulla, with statistical significance values also reaching p<0.0001. These results suggest relevant morphological variations in the adrenal gland among the analyzed groups.

Table 3. Histological evaluation of the kidney and adrenal gland in female Sprague Dawley rats exposed to PM2.5

	Kidney			Adrenal gland			
Group	A	B	C	D	E	F	G
FA/FA	+++	+++	+++	+++	---	+++	+--
FA/NFA	+ -	+++	++-	++-	--+	++-	+++
NFA/FA	- -	++-	---	+- -	++-	+--	++-
NFA/NFA	- - -	+--	+--	---	+++	---	---

A: Compactness of the glomeruli in the renal corpuscle. B: Epithelial preservation of the proximal convoluted tubule (PCT). C: Extension of the medullary ray (MR). D: Homogeneity of cell cytoplasm in the zona fasciculata (ZF). E: Dilation of cortical blood vessels. F: Drainage of blood vessels into the medullary sinuses. G: Nuclear size in chromaffin cells.

Table 4. Morphometry and stereology (mean ± S.D.) of the kidney in female Sprague Dawley rats exposed to PM2.5 from wood smoke

	FA/FA	FA/NFA	NFA/FA	NFA/NFA	p-value
Kidney (ml)	1.200 ± 0.232	0.910 ± 0.237	1.050 ± 0.154	1.240 ± 0.116	0.1152
Cortex (ml)	0.803 ± 0.094	0.635^{AB} ± 0.053	0.747^{C} ± 0.071	0.878^{BC} ± 0.061	<0.0001
Medulla (ml)	0.397^{A} ± 0.094	0.265^{A} ± 0.053	0.297 ± 0.073	0.362 ± 0.061	0.0131
V_V (%) cortex	66.913 ± 7.832	70.245 ± 5.632	71.360 ± 6.929	70.826 ± 5.005	0.6127
V_V (%) medulla	33.087 ± 7.832	29.754 ± 5.633	28.623 ± 6.925	29.174 ± 5.005	0.6111
V_V (%) Glo	15.273 ± 6.856	16.662 ± 5.428	13.426 ± 5.782	17.708 ± 6.076	0.3030
V_V (%) Glo/kidney	0.178 ± 0.078	0.148^{A} ± 0.048	0.141^{B} ± 0.060	0.220^{AB} ± 0.076	0.0124
S_V Glo ($\mu m^2/\mu m^3$)	0.007 ± 0.005	0.010^{A} ± 0.004	0.006^{A} ± 0.003	0.008 ± 0.002	0.0701
S_V Glo/kidney (μm^2)	8.900 ± 6.171	9.229 ± 3.522	5.955^{A} ± 3.278	10.250^{A} ± 2.206	0.0474
N_V (Glo/μm^2)	0.125 ± 0.049	0.145 ± 0.047	0.120 ± 0.052	0.157 ± 0.054	0.2027

Similar letters indicate statistical differences between groups. Glo: glomerulus. Statistical analyses were conducted using ANOVA with Tukey's *post-hoc* test to discern significant differences among groups.

Table 5. Stereology (mean ± S.D.) of the adrenal gland in female Sprague Dawley rats subjected to PM2.5 from wood smoke.

	FA/FA	FA/NFA	NFA/FA	NFA/NFA	*p*-value
V_V (%) cortex	$67.494^{ABC} \pm 5.441$	$58.048^{A} \pm 7.127$	$56.393^{B} \pm 5.429$	$51.567^{C} \pm 4.047$	<0.0001
V_V (%) medulla	$32.121^{ABC} \pm 5.761$	$41.944^{A} \pm 7.130$	$43.607^{B} \pm 5.429$	$48.433^{C} \pm 4.047$	<0.0001
V_V (%) SCE	$87.347^{AC} \pm 6.995$	$89.932^{BD} \pm 7.577$	$78.836^{AB} \pm 9.265$	$70.815^{CD} \pm 10.370$	<0.0001
S_V SCE ($\mu m^2/\mu m^3$)	0.024 ± 0.014	$0.027^{A} \pm 0.011$	$0.015^{A} \pm 0.008$	0.018 ± 0.010	0.0075
N_V (SCE/μm^2)	2.372 ± 1.256	2.095 ± 1.092	1.626 ± 0.742	2.111 ± 1.100	0.2909

Similar letters indicate statistical differences between groups. Glo: glomerulus. Statistical analyses were conducted using ANOVA with Tukey's *post-hoc* test to discern significant differences among groups.

4. DISCUSSION

We hypothesized that chronic exposure to PM2.5 from wood smoke during pregestational and gestational stages has an adverse effect on the morphology of the kidney and adrenal gland. The findings showed significant microscopic structural changes in both organs, without affecting macroscopic characteristics. PM2.5 exposure resulted in histological modifications that could influence the GFR, indicating a metabolic adaptation to the contaminated environment. This phenomenon was reflected in an increase in the number of glomeruli in the renal cortex, suggesting a possible pathological state and potential kidney disease. In the adrenal gland, hypertrophy and hyperplasia were observed in the zona fasciculata, indicating a functional alteration of the SCE in response to elevated metabolic demands. The proportional decrease in SCE and the increase in the proportion of adrenal medulla suggest an adaptive response to continuous PM2.5 exposure. PM2.5 exposure from wood smoke significantly impacted renal and adrenal morphology in pregnant rats. The control groups (FA/FA), exposed only to filtered air, showed the least structural alteration, implying protection against PM2.5. The groups exposed to unfiltered air, especially during both pregestational and gestational stages (NFA/NFA), presented more pronounced morphological changes, with increases in arteriole diameter and variations in the density and volume of renal and adrenal tissues, suggesting possible adaptation mechanisms or responses to PM2.5-induced damage. This pattern suggests vascular and morphological adaptations that could affect renal and endocrine function. The findings highlight the need for further investigation into the impact of air quality on renal and endocrine health, and the importance of mitigating environmental contaminant exposure during critical developmental stages, such as gestation, to preserve the structural and functional integrity of vital organs.

4.1 PM2.5 derived from wood smoke and its structural effects on the kidney

Histological findings demonstrate the harmful effects of chronic PM2.5 exposure during pregestational and gestational stages in female Sprague Dawley rats. The group exposed to PM2.5 at both stages (NFA/NFA) showed the most significant morphological changes, with a marked deterioration in the glomerular, tubular, and medullary ray structures compared with the control group (FA/FA). The decrease in glomerular compactness and dilation of urinary spaces indicate potential dysfunctions in the renal filtration process. Additionally, changes in the morphology of the PCT, such as anastomosed cells and loss of typical structure, suggest impaired reabsorption and secretion capacity. Although the integrity of the Loop of Henle was maintained, progressive increases in the diameter of cortical arterioles point to a vascular adaptive response to a stressful environment. These findings underscore the vulnerability of the kidney and adrenal gland to environmental contaminants during critical developmental periods and reinforce the need for strategies to mitigate air pollution exposure to safeguard renal and endocrine health. PM2.5 derived from wood smoke did not affect kidney volume, consistent with studies indicating that kidney size depends on multiple variables, such as height, age, hydration status, pregnancy, renal mass loss, smoking, and intra- and inter-observer variability (García et al., 2023). Zhao et al. (2020) reported that in pregnant women in China, exposure to PM2.5 and its chemical components was associated with a reduction in the estimated GFR (eGFR), evidencing the nephrotoxicity of PM2.5. Research in the general population also indicates that long-term exposure to PM2.5 is linked to reduced renal function and an increased risk of chronic kidney disease (Yang et al., 2016). Fang et al. (2020) found significant associations between personal PM2.5 exposure and adverse changes in eGFR in older individuals. Improving air quality and reducing PM2.5 levels have been associated with a lower risk of developing chronic kidney disease (Bo et al., 2021).

García et al. (2023) highlighted that an increase in the size of the nephron and kidney can trigger adverse cellular responses, such as glomerular activation, fibrosis, and vasoconstriction, resulting in hypertension and long-term kidney damage. Although PM2.5 exposure did not directly affect renal volume, adaptive processes like autophagy may play a crucial role in the self-regulation of kidney damage, preventing renal failure (Huang et al., 2020). Xu et al. (2023) suggested that macrophages can phagocytize PM2.5 particles, impacting the immune and inflammatory response in the kidney. Susceptibility to PM2.5-induced nephropathy may also be influenced by specific genetic polymorphisms (Katakami et al., 2013). Studies in patients with Fabry disease suggest that metabolic disorders and exposure to contaminants can interact, exacerbating kidney damage (Rombach et al., 2010). Exposure to PM2.5 has a significant impact on kidney structure, especially during gestation. Although PM2.5 from wood smoke does not affect the number of glomeruli in the renal cortex (Nv [Glo/μm^2]), the group exposed before and during gestation (NFA/NFA) showed a higher number of glomeruli, suggesting an adaptive response to increase the GFR. Studies on the increase in the proportion of glomeruli or the GFR associated with PM2.5 exposure are scarce. Studies by Carracedo and Ramírez (2020) and Carrillo-Mora et al. (2021) showed how changes in renal structure can influence its function. The increase

in the proportion of glomeruli (Vv % Glo/kidney) in the group exposed to PM2.5 (NFA/NFA) suggests an increase in the GFR, implying greater renal functionality (Carracedo and Ramírez, 2020). Carrillo-Mora et al. (2021) reported that 80% of pregnant mothers present physiological hydronephrosis, increasing kidney volume; vascular changes increase plasma flow and GFR. PM2.5 exposure affected the surface area of glomeruli in the renal cortex (Sv Glo ($\mu m^2/\mu m^3$)) and their total surface area (Sv Glo/kidney (μm^2)). Increased glomerular surface area can lead to glomerular hyperfiltration, with a GFR higher than normal (Yang and Xu, 2022). This increase is related to adaptation to increased body surface area, as in obesity, resulting in a larger kidney size (Afsra et al., 2019). The adaptation and potential kidney damage from PM2.5 exposure, along with factors like physiological hydronephrosis during pregnancy, highlight the complexity of renal responses to various conditions. Glomerular hyperfiltration, although adaptive, may also indicate a risk of chronic kidney diseases.

Even though PM2.5 did not show an effect on the proportion of cortex in the kidney (Vv % cortex), the analysis of total cortical volume revealed differences between groups. This was particularly evident in groups that inhabited mixed environments before and during gestation, while groups exposed to an unfiltered environment throughout the entire period showed no differences. This finding suggests a structural effect on the kidney from transitioning between filtered and unfiltered environments (and *vice versa*). The effect of stress on renal physiology could explain this. According to Marchon et al. (2018), prepubertal rats subjected to stress showed reductions in kidney weight, kidney volume, cortical volume, glomerular volume fraction (Vv (%) Glo), and the number of glomeruli. Xu et al. (2023) reported that PM2.5 exposure showed an increase in kidney weight along with cortical enlargement. According to Yariwake et al. (2021), this increase may be associated with nephron hypertrophy, characterized by large glomeruli and dilated tubules, which relates to a higher GFR and proteinuria. García et al. (2023) noted that the progressive reduction of the renal cortex and the relative saving of medullary volume through tubular hypertrophy compensate for alterations such as sclerosis and atrophy of the superficial nephrons. Changes in cortical proportion are common findings in chronic renal alterations such as vascular nephropathy, which manifests as cortical thinning, arterial hypertension, and progressive renal failure (Alamillo et al., 2007).

In our study, PM2.5 exposure from wood smoke impacted the proportion of medulla in the kidney (Vv % medulla/kidney), especially in the FA/FA and FA/NFA groups. The modification of renal parenchymal volume is related to the inflammatory response, a rapid immune reaction to eliminate toxins and promote recovery. However, prolonged inflammation hinders the body's functioning (Xu et al., 2022). León Regal et al. (2015) indicated that inflammation can increase the proportion of renal parenchyma, which is associated with greater vascular permeability and vasodilation. PM2.5 exposure can cause renal injury or dysfunction by crossing the gas-blood barrier, accumulating in the kidneys, and activating humoral and cellular inflammatory mediators, damaging endothelial cells and affecting renal microcirculation (Xu et al., 2022). Additionally, podocytes stimulated by PM2.5 release inflammatory cytokines, aggravating the inflammatory response and

causing cellular damage. Kronbichler et al. (2017) indicated that PM2.5 disintegrates F-actin fibers, altering the integrity of the cytoskeleton and nuclear structure, leading to structural adaptations in the renal parenchyma.

4.2 PM2.5 derived from wood smoke and its structural effects on the adrenal gland

The zona fasciculata, constituting 80% of the cortical volume, showed notable variations between groups. The FA/FA group rats, exposed to filtered air pregestationally and gestationally, displayed consistent cellular organization and homogeneous cytoplasmic content, with acidophilia and abundant lipid inclusions, as seen in previous studies (Rosol et al., 2001; Zaki et al., 2018). In contrast, NFA/NFA rats, exposed to unfiltered air, showed reduced acidophilia and lipid content, with less cytoplasmic homogeneity and empty spaces, indicating altered adrenal function (Castro et al., 2009). Reduced acidophilia suggests fewer proteins and enzymes for steroid hormone synthesis (Afsar et al., 2019), and reduced lipid content indicates less accumulation of necessary lipids (Zarobkiewicz et al., 2018). Cytoplasmic heterogeneity and empty spaces suggest cellular damage and lipid storage dysfunction. These changes may compromise the adrenal gland's ability to synthesize and secrete essential hormones like cortisol, affecting stress regulation and metabolism, as studies on environmental contaminant toxicities indicate (Bazeliuk, 2003; Koko et al., 2004; El-Tahawy and Abozaid, 2019). The FA/NFA and NFA/FA groups showed intermediate characteristics, suggesting an accumulative and persistent impact of PM2.5 on adrenal structure. Cortical blood vessels showed differences in fenestrated sinusoidal capillaries. FA/FA rats had capillaries with compressed endothelial nuclei and dilated lumens, while NFA/NFA rats showed non-compressed nuclei and dilated lumens, suggesting an accumulative contaminant effect (Fujita et al., 2008). The nuclei of MCC in FA/FA rats were smaller and basophilic, while in NFA/NFA rats, they were larger and basophilic, reflecting a high rate of protein synthesis and possible adaptation to chronic contaminant exposure (Liu et al., 2004). The proportion of SCE (Vv % SCE) also differed between groups, likely due to PM2.5-induced stress, affecting SCE morphology and function (Ulrich-Lai et al., 2006; Li et al., 2017). PM2.5 significantly affected the area of SCE in the zona fasciculata. Pan et al. (2021) mentioned that PM2.5 exposure increases surrounding stress hormones, implicating the hypothalamic-pituitary-adrenal (HPA) axis in the pathogenesis of air pollution's systemic adverse effects. As Ulrich-Lai et al. (2006) stated, an increase in SCE surface area (Sv SCE [$\mu m^2/\mu m^3$]) demonstrates the high demand for the synthesis and secretion of corticosterone released in response to chronic stress, providing more space for the hormone's synthesis and secretion.

PM2.5 exposure affected both the cortex proportion (Vv % cortex) and medulla proportion (Vv % medulla). According to Ying et al. (2014), prolonged PM2.5 exposure may contribute to hypothalamic inflammation, resulting in severe metabolic disorders and homeostasis imbalance. Balasubramanian et al. (2013) suggested that the stress axis can adapt to repeated stressful episodes, indicating that the lack of significant norepinephrine (NE) increases after multiple PM2.5 exposure is part of an adaptive response. Bozzo et al. (2011) mentioned that mental conditions like pharmacological manipulation, castration, or unilateral adrenalectomy induce increased cell proliferation in the adrenal cortex. According to Guerrero (2017), Hans

Seyle's early work showed that organisms develop an alarm reaction to damage. His experimental results showed that adrenal glands increased in size with lipid discharge and loss of chromaffinity in the adrenal medulla.

While our study shows that PM2.5 induces structural changes in the adrenal gland, the literature describes the pathophysiological changes in the adrenal gland in response to PM2.5. According to Liu et al. (2020), a mechanism by which PM2.5 activates the HPA axis is PM2.5-induced neuroinflammation, affecting central nervous system pathways that can stimulate the HPA axis. HPA activation promotes the secretion of corticotropin-releasing hormone (CRH) from the hypothalamus, stimulating the pituitary to secrete ACTH, which is released into the circulatory system and acts on the adrenal glands to promote corticosterone secretion. According to García et al. (2023), the inflammatory state is the most common response to PM2.5 exposure, with its chemical compounds linked to systemic changes that can trigger and/or worsen various pathological conditions. Feng et al. (2023) mentioned that chemicals coated on PM2.5 can alter the integrity of multiple physiological barriers and translocate from the lung to systemic circulation, accessing various secondary target organs, including the heart, kidney, liver, spleen, lymph nodes, and brain in humans and animal models. According to Li et al. (2019), the interaction of PM2.5 from wood smoke with the respiratory tract induces the formation of pro-inflammatory molecules such as interleukins (IL) 1, 2, 6, 7, and TNF (tumor necrosis factor) and local pro-oxidants that affect other organs and alter tissue function. PM2.5 modifies cellular biomolecules and activates the immune response, beginning with the recruitment of immune cells and the production of cytokines that promote pro-inflammatory signaling. Bekki et al. (2016) mentioned that macrophages play a fundamental role in defense against inhaled particles through phagocytosis and cytokine and chemokine release, causing inflammation in lung tissue. ROS are key in defense, and ROS production results in oxidative stress, damaging lung cells and structures and triggering respiratory diseases. Feng et al. (2023) mentioned that PM2.5-mediated ROS can react with biomacromolecules, altering their structure and function. These inflammatory mechanisms and ROS generation could explain the structural changes observed in the kidney, such as the increased number of glomeruli and the increase in the renal cortex, and in the adrenal gland, such as the decreased proportion of SCE and increased proportion of adrenal medulla in pregnant females during gestation.

4.3 Study limitations

One limitation of this study was the use of an animal model, which may not fully replicate human responses to PM2.5 exposure. Rats were selected due to their extensive and validated use in environmental toxicology studies, and results from similar studies were considered to contextualize our findings. Although rats were exposed to filtered and unfiltered air conditions, real-world environmental contaminant exposure variability can be much higher, complicating direct extrapolation to humans. This limitation was mitigated by a controlled experimental design, allowing direct comparisons between different exposure groups. The duration and intensity of exposure in the study may not reflect chronic human conditions. An exposure protocol was

designed to mimic real environmental pollution conditions, using PM2.5 concentrations representative of highly polluted areas. Another limitation is the exclusive evaluation of renal and adrenal morphology without a detailed functional exploration. This was addressed by detailed quantitative (stereology) and histological analyses to provide information on significant structural changes. Anatomically, the human adrenal gland is located above the kidney, while in rats, it is in the cranial region. This difference may influence the response to contaminants due to blood flow distribution and dynamics. To address this, our results were compared with previous studies in humans and other animal models. Finally, the limitation in the number of animals per group could affect the statistical robustness of the findings. A rigorous experimental design and appropriate statistical analyses were used to ensure the validity of the results. Future research should include a larger sample size and complementary functional analyses to validate and expand these results.

In conclusion, exposure to PM2.5 derived from wood smoke has significant effects on the morphology of both the kidney and adrenal gland in pregnant female rats. Our study demonstrates that these effects are more pronounced when exposure occurs both pregestationally and gestationally. In this group, the rats showed notable alterations in the kidney, such as glomerular compactness, PCT morphology, and medullary ray structure, suggesting dysfunctions in renal filtration and reabsorption and secretion capacity. In the adrenal gland, there was a decrease in acidophilia and lipid content in the zona fasciculata, along with cytoplasmic heterogeneity and the appearance of empty spaces, indicating altered adrenal function. These findings suggest that combined pregestational and gestational exposure to PM2.5 has an accumulative and persistent impact on the structure of these organs. Therefore, air quality during these critical periods is crucial for maternal-fetal health, and mitigation strategies should be implemented to reduce exposure to environmental contaminants and protect the structural and functional integrity of vital organs. These results support the need for public policies focused on improving air quality and reducing PM2.5 exposure, especially in areas where wood burning is common for heating.

DECLARATIONS

Competing Interests Statement

The authors declare that they have no competing interests.

ORCID

Paulo Salinas https://orcid.org/0000-0003-2273-0904

Francisca Villarroel https://orcid.org/0009-0008-6643-5935

Carlos González-Torres https://orcid.org/0000-0002-7765-6388

Aliro Maulen https://orcid.org/0009-0001-4131-735X

Eva Rojas https://orcid.org/0000-0001-6526-8321

Ethics approval

Scientific Ethics Committees of the University de La Frontera (Act 122/20) and the Bioethics and Biosafety Committee of the Pontificia Universidad Católica de Valparaíso (Act BIO EPUCV-BA 373-2020)

Data Availability Statement

The data that support the findings of this study are available from the corresponding author upon reasonable request.

Acknowledgment

ANID- Fondecyt 11200775 (Paulo Salinas)

Funding

This research received no specific grant from funding agencies in the public, commercial, or not-for-profit sectors.

Authors' contribution

The study was conceived and designed by Paulo Salinas (PS). Histological techniques and descriptions were performed by Aliro Maulen (AM) and Eva Rojas (ER), while stereological analyses were conducted by Francisca Villarroel (FV), Carlos González (CG), Tamara Lazcano (TL), and Jovely Silva (JS). Data collection and the drafting of the initial manuscript were collaborative efforts by PS, AM, ER, FV, CG, TL, and JS. All authors contributed to data analysis and discussion of the results and approved the final manuscript. PS was responsible for supervising the study.

Funding

No funds, grants, or other support was received.

REFERENCES

Afsar B., Elsurer Afsar R., Kanbay A., Covic A., Ortiz A. and Kanbay M. (2019). Air pollution and kidney disease: review of current evidence. Clin. Kidney J. 12, 19-32.

Alamillo C.G., Fresnedo G.F., San Millán J.C.R. and Rodríguez M.A.A. (2007). Nefropatías vasculares. Med. Programa Form. Médica Contin. Acreditado 9, 5283-5289.

Alsuwaida A., Mousa D., Al-Harbi A., Alghonaim M., Ghareeb S. and Alrukhaimi M.N. (2011). Impact of early chronic kidney disease on maternal and fetal outcomes of pregnancy. J. Matern. Fetal Neonatal Med. 24, 1432-1436.

Balasubramanian P., Sirivelu M.P., Weiss K.A., Wagner J.G., Harkema J.R., Morishita M., Mohankumar P.S. and Mohankumar S.M. (2013). Differential effects of inhalation exposure to PM2.5 on hypothalamic monoamines and corticotrophin releasing hormone in lean and obese rats. Neurotoxicology, 36, 106-111.

Bazeliuk L.T. (2003). Cytomorphological and metabolic changes in the adrenal glands of rats exposed to coal and rock dust and during exercise. Gig. Sanit. 55-57. (article in Russian).

Beers K. and Patel N. (2020). Kidney physiology in pregnancy. Adv. Chronic Kidney Dis. 27, 449-454.

Bekki K., Ito T., Yoshida Y., He C., Arashidani K., He M., Sun G., Zeng Y., Sone H., Kunugita N. and Ichinose T. (2016). PM2.5 collected in China causes inflammatory and oxidative stress responses in macrophages through the multiple pathways. Environ. Toxicol. Pharmacol. 45, 362-369.

Blanco E., Rubilar F., Quinteros M.E., Cayupi K., Ayala S., Lu S., Jimenez R. B., Cárdenas J. P., Blazquez C. A., Delgado-Saborit J. M., Harrison R. M. and Ruiz-Rudolph P. (2022). Spatial distribution of particulate matter on winter nights in Temuco, Chile: Studying the impact of residential wood-burning using mobile monitoring. Atmos. Environ. 286, 119255.

Bo Y., Brook J.R., Lin C., Chang L.Y., Guo C., Zeng Y., Yu Z., Tam T., Lau A. K.H. and Lao X.Q. (2021). Reduced ambient $PM_{2.5}$ was associated with a decreased risk of chronic kidney disease: A longitudinal cohort study. Environ. Sci. Technol. 55, 6876-6883.

Bozzo A.A., Soñez C.A., Monedero Cobeta I., Rolando N.A., Romanini M.C., Lazarte M. and Ávila R. (2011). Chronic stress effects on adrenal cortex cellular proliferation in pregnant rats. Int. J. Morphol. 29, 1148-1157.

Carracedo J. and Ramírez R. (2020). Fisiología renal. Soc. Española Nefrol. 1-20.

de Castro K.R., Almeida G.H.D.R., Matsuda M., de Paula Vieira R., Martins M.G., Rici R.E.G., Saldiva P.H.N. and Veras M.M. (2024). Exposure to urban ambient particles (PM2.5) before pregnancy affects the expression of endometrial receptive markers to embryo implantation in mice: Preliminary results. Tissue Cell 88, 102368

Dorph-Petersen K.A., Nyengaard J.R. and Gundersen H.J. (2001). Tissue shrinkage estimation in stereology. J. Microsc. 20, 232-246.

El-Tahawy N.F.G. and Abozaid S.M.M. (2019). The possible structural changes in the adrenal gland cortex after induction of hepatic ischemia-reperfusion injury in male albino rats: Light and electron microscopic study. J. Cell. Physiol. 234, 15487-15495

Fang J., Tang S., Zhou J., Zhou J., Cui L., Kong F., Gao Y., Shen Y., Deng F., Zhang Y., Liu Y., Dong H., Dong X., Dong L., Peng X., Cao, M., Wang Y., Ding C., Du Y., Wang Q., Wang C., Zhang Y., Wang Y., Li T. and Shi X. (2020). Associations between personal $PM_{2.5}$ elemental constituents and decline of kidney function in older individuals: The China BAPE study. Environ. Sci. Technol. 54, 13167-13174.

Feng S., Huang F., Zhang Y., Feng Y., Zhang Y., Cao Y. and Wang X. (2023). The pathophysiological and molecular mechanisms of atmospheric $PM_{2.5}$ affecting cardiovascular health: A review. Ecotoxicol. Environ. Saf. 249, 114444.

Fujita K., Ito H., Nakano S., Kinoshita Y., Wate R. and Kusaka H. (2008). Immunohistochemical identification of messenger RNA-related proteins in basophilic inclusions of adult-onset atypical motor neuron disease. Acta Neuropathol. 116, 439-445.

García A., Santa-Helena E., De Falco A., de Paula Ribeiro J., Gioda A. and Gioda C.R. (2023). Toxicological effects of fine particulate matter ($PM_{2.5}$): Health Risks and Associated systemic injuries-systematic review. Water Air Soil Pollut. 234, 346.

Guerrero J. (2017). Para entender la acción de cortisol en inflamación aguda: una mirada desde la glándula suprarrenal hasta la célula blanco. Rev. Med. Chil. 145, 230-239.

Gundersen H.J.G., Bendtsen T.F., Korbo L., Marcussen N., Møller A., Nielsen K., Nyengaard J.R., Pakkenberg B., Sørensen F.B., Vesterby A. and West M.J. (1988). New stereological methods for pathology. APMIS 96, 379-394.

Huang X., Zhou Z., Liu X., Li J. and Zhang L. (2020). PM2.5 exposure induced renal injury via the activation of the autophagic pathway in the rat and HK-2 cell. Environ. Sci. Eur. 32, 1-13.

International Committee on Veterinary Histological Nomenclature (ICVHN). (2017). Nomina Histologica Veterinaria. Web Site, World Association Veterinary Anatomists. Available from: https://www.wava-amav.org/downloads/NHV_2017.pdf

IQAir (2019. Most Polluted Cities In The World In 2021: Ranking PM2.5 | IQAir, Iqair.com, n.d. https://www.iqair.com/es/world-most-polluted-cities

IQAir (2022). First in Air Quality. (2022). https://www.iqair.com/world-air-quality-report

Katakami N., Kume S., Kaneto H., Uzu T., Kashiwagi A., Yamasaki Y., Maegawa H. and Shimomura I. (2013). Association of myeloperoxidase G-463A gene polymorphism with diabetic nephropathy in Japanese type 2 diabetic subjects. Endocr. J. 60, 457-471.

Koko V., Djordjeviae J., Cvijiae G. and Davidoviae V. (2004). Effect of acute heat stress on rat adrenal glands: a morphological and stereological study. J. Exp. Biol. 207, 4225-4230.

Levin G., Elchalal U. and Rottenstreich A. (2019). The adrenal Cortex: Physiology and diseases in human pregnancy. Eur. J. Obstet. Gynecol. Reprod. Biol. 240, 139-143.

Li H., Cai J., Chen R., Zhao Z., Ying Z., Wang L., Chen J., Hao K., Kinney P.L., Chen H. and Kan H. (2017). Particulate matter exposure and stress hormone levels: a randomized, double-blind, crossover trial of air purification. Circulation 136, 618-627.

Li Y., Xu H., He K., Wang J., Ning Z., Wang Q., Li N., Shen Z., Liu P., Sun J., Niu X., Cao Y. and Cao J. (2019). Reactive oxygen species induced by personal exposure to fine particulate matter emitted from solid fuel combustion in rural Guanzhong Basin, northwestern China. Air Qual. Atmos. Health 12, 1323-1333.

Liu J., Li X.D., Vaheri A. and Voutilainen R. (2004). DNA methylation affects cell proliferation, cortisol secretion and steroidogenic gene expression in human adrenocortical NCI-H295R cells. J. Mol. Endocrinol. 33, 651-662.

Liu C., Yang J., Guan L., Zhu Y. and Geng X. (2020). Filtered air intervention reduces inflammation and hypothalamus-pituitary-adrenal axis activation in adult male and female rats after PM2.5 exposure. Environ. Sci. Pollut. Res. 27, 35341-35348.

Marchon R.G., Ribeiro C.T., Costa W.S., Sampaio F.J.B., Pereira-Sampaio M.A. and de Souza D.B. (2018). Immediate and late effects of stress on kidneys of prepubertal and adult rats. Kidney Blood Press. Res. 43, 1919-1926.

Mehta A.J., Zanobetti A., Bind M.A.C., Kloog I., Koutrakis P., Sparrow D., Vokonas P. S. and Schwartz J.D. (2016). Long-term exposure to ambient fine particulate matter and renal function in older men: the veterans administration normative aging study. Environ. Health Perspect. 124, 1353-1360.

699 Nyengaard J.R. (1999). Stereologic methods and their application in kidney research. J. Am. Soc. Nephrol. 10, 1100-
700 1123.
701 Pan B., Chen M., Zhang X., Liang S., Qin X., Qiu L., Cao Q., Peng R., Tao S., Li Z., Zhu Y., Kan H., Xu Y. and
702 Ying Z. (2021). Hypothalamic-pituitary-adrenal axis mediates ambient $PM_{2.5}$ exposure-induced pulmonary
703 inflammation. Ecotoxicol. Environ. Saf. 208, 111464.
704 Rombach S., Baas M., Berge I., Krediet R., Bemelman F. and Hollak C. (2010). The value of estimated GFR in
705 comparison to measured GFR for the assessment of renal function in adult patients with Fabry disease. Nephrol.
706 Dial. Transplant. 25, 2549-2556.
707 Rosol T.J., Yarrington J.T., Latendresse J. and Capen C.C. (2001). Adrenal gland: structure, function, and
708 mechanisms of toxicity. Toxicol. Pathol. 29, 41-48.
709 Salinas P., Veuthey C., Rubio I., Bongiorno A. and Romero I. (2020). Exposure to wood smoke pollution during
710 pre-gestational period of rat has effects on placenta volume and fetus size. Int. J. Morphol. 38, 1356-1364.
711 Santos U.D.P., Arbex M.A., Braga A.L.F., Mizutani R.F., Cançado J.E.D., Terra-Filho M. and Chatkin J.M. (2021).
712 Environmental air pollution: respiratory effects. J. Bras. Pneumol. 47, e20200267.
713 Tschanz S.A., Burri P.H. and Weibel E.R. (2011). A simple tool for stereological assessment of digital images: the
714 STEPanizer. J. Microsc. 243, 47-59.
715 Ulrich-Lai Y.M., Figueiredo H.F., Ostrander M.M., Choi D.C., Engeland W.C. and Herman J.P. (2006). Chronic
716 stress induces adrenal hyperplasia and hypertrophy in a subregion-specific manner. Am. J. Physiol. Endocrinol.
717 Metab. 291, E965-E973.
718 Van Koppen A., Verhaar M.C., Bongartz L.G. and Joles J.A. (2013). 5/6th nephrectomy in combination with high
719 salt diet and nitric oxide synthase inhibition to induce chronic kidney disease in the Lewis rat. J. Vis. Exp. 77,
720 e50398.
721 Villarroel F., Ponce N., Gómez F.A., Muñoz C., Ramírez E., Nualart F. and Salinas P. (2024). Exposure to fine
722 particulate matter 2.5 from wood combustion smoke causes vascular changes in placenta and reduce fetal size.
723 Reprod. Toxicol. 127, 108610.
724 World Health Organization: WHO. (2022). Contaminación del aire ambiente (exterior).
725 https://www.who.int/es/news-room/fact-sheets/detail/ambient-(outdoor)-air-quality-and-health
726 Xie G., Wang R., Yang W., Sun L., Xu M., Zhang B., Yang L., Shang L., Qi C. and Chung M.C. (2022). Associations
727 among prenatal $PM_{2.5}$, birth weight, and renal function. Chemosphere 301, 134668.
728 Xu C., Zhang Q., Huang G., Huang J. and Zhang H. (2023). The impact of PM2.5 on kidney. J. Appl. Toxicol. 43,
729 107-121.
730 Xu W., Wang S., Jiang L., Sun X., Wang N., Liu X. Yao X., Qiu T., Zhang C., Li J., Deng H. and Yang G.
731 (2022). The influence of $PM_{2.5}$ exposure on kidney diseases. Hum. Exp. Toxicol. 41, 9603271211069982.
732 Yang Y. and Xu G. (2022). Update on pathogenesis of glomerular hyperfiltration in early diabetic kidney
733 disease. Front. Endocrinol. 13, 872918.
734 Yang Y., Chen Y., Chen S. and Chan C. (2016). Associations between long-term particulate matter exposure and
735 adult renal function in the Taipei Metropolis. Environ. Health Perspect. 125, 602-607.

Yariwake V.Y., Torres J.I., Dos Santos A.R.P., Freitas S.C.F., De Angelis K., Farhat S.C.L., Câmara N.O.S and Veras M.M. (2021). Chronic exposure to PM2.5 aggravates SLE manifestations in lupus-prone mice. Part. Fibre Toxicol. 18, 1-16.

Ying Z., Xu X., Bai Y., Zhong J., Chen M., Liang Y., Zhao J., Liu D., Morishita M., Sun Q., Spino C., Brook R.D., Harkema J.R. and Rajagopalan S. (2014). Long-term exposure to concentrated ambient PM2.5 increases mouse blood pressure through abnormal activation of the sympathetic nervous system: A role for hypothalamic inflammation. Environ. Health Perspect. 122, 79-86.

Zaki S.M., Abdelgawad F.A., El-Shaarawy E.A.A., Radwan R.A.K. and Aboul-Hoda B.E. (2018). Stress-induced changes in the aged-rat adrenal cortex. Histological and histomorphometric study. Folia Morphol. 77, 629-641.

Zarobkiewicz M.K., Woźniakowski M.M., Wawryk-Gawda E., Sławiński M.A., Halczuk P., Korolczuk A. and Jodłowska-Jędrych B. (2018). Decrease in lipid droplets in adrenal cortex of male Wistar rats after chronic exposure to energy drinks. Medicina (Kaunas) 54, 90.

Zhao Y., Cai J., Zhu X., Donkelaar A., Martin R., Hua J. and Kan H. (2020). Fine particulate matter exposure and renal function: A population-based study among pregnant women in China. Environ. Int. 141, 105805.

Zhu N., Ji X., Geng X., Yue H., Li G. and Sang N. (2021). Maternal $PM_{2.5}$ exposure and abnormal placental nutrient transport. Ecotoxicol. Environ. Saf. 207, 111281.

LIST OF FIGURES

Figure 1. Exposure chamber design and experimental groups. **(A)** Filtered Air Chamber (FA). **(B)** Non-Filtered Air Chamber (NFA). **(C)** Experimental design and exposure groups. Rattus norvegicus from the G0 generation were exposed to either filtered or non-filtered air. Their offspring (G1) were also raised in the same conditions and subsequently mated to produce the G2 generation. G2 females were exposed to filtered or non-filtered air during the pregestational period and were then divided into four groups based on the gestational period exposure: FA/FA, FA/NFA, NFA/FA, and NFA/NFA. After the gestational period, a celiotomy was performed to remove the kidneys and adrenal glands for further analysis.

Figure 2. Test system M_{36} point grid in transverse sections and kidney cortex. **(A)** Transverse section of the kidney showing the use of the M_{36} point grid system for the stereological evaluation of renal structure. The points indicate the intersections used for quantitative analysis. **(B)** Enlarged image of the renal cortex, highlighting the application of the M_{36} line grid system for the evaluation of glomeruli and convoluted tubules.

Figure 3. Histological analysis of kidney and adrenal gland in female Sprague Dawley rats exposed to PM2.5. **(A-C)** Sections of the kidney and **(D-E)** adrenal gland from different exposure groups: FA/FA, FA/NFA, NFA/FA and NFA/NFA. Kidney: **(A)** High-magnification images of glomeruli (white arrowhead) and convoluted tubules (asterisks) in the renal cortex. **(B)** The distal portion of the loop of Henle (black arrowheads). Brush borders of the distal convoluted tubules (white arrowheads). **(C)** High-magnification images of the renal medulla highlighting collecting tubules (black arrows), a thin portion of the loop of Henle

(asterisks), and an ascending portion of the loop of Henle (black arrows). Adrenal gland: **(D**) Low-magnification images of the adrenal gland, showing the zona glomerulosa (zg), zona fasciculata (zf), zona reticularis (zr), and medulla (med). White arrowheads indicate blood vessels in the medulla. **(E)** High-magnification images of the zona fasciculata, with black arrowheads indicating the nuclei of spongy cortical endocrinocytes (SCE). (Stain: hematoxylin-eosin). Scale bars are 800 μm and 400 μm in the panoramic images at the top, 50 μm in (A) and (C), 100 μm in (B) and (D), and 50 μm in (E).

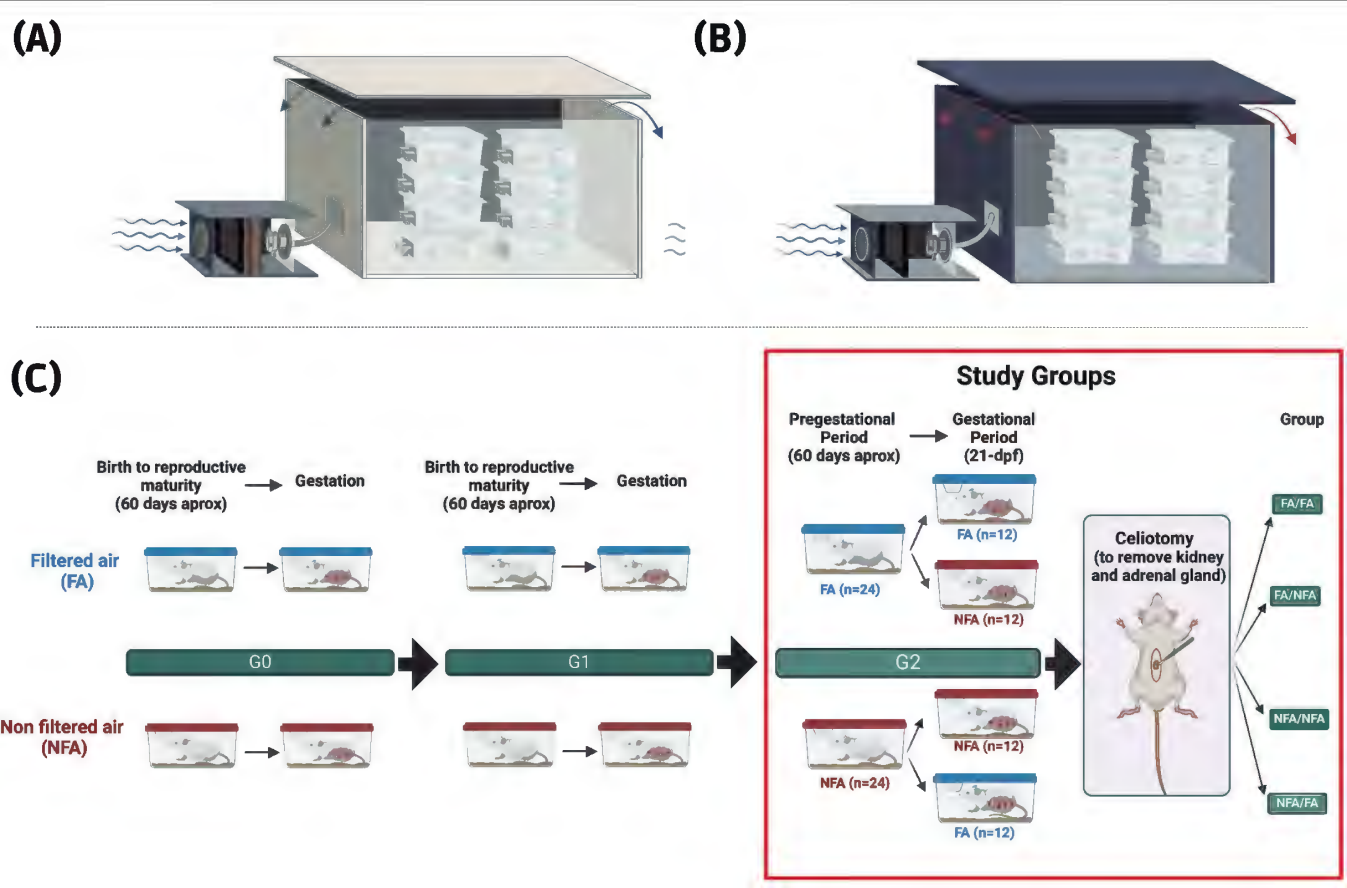
(A)
(B)
(C)
Birth to reproductive maturity (60 days aprox)
Gestation
Birth to reproductive maturity (60 days aprox)
Gestation
Filtered air (FA)
G0
G1
Non filtered air (NFA)
Study Groups
Pregestational Period (60 days aprox)
Gestational Period (21-dpf)
Group
FA (n=24)
FA (n=12)
NFA (n=12)
G2
Celiotomy (to remove kidney and adrenal gland)
NFA (n=24)
NFA (n=12)
FA (n=12)
FA/FA
FA/NFA
NFA/NFA
NFA/FA

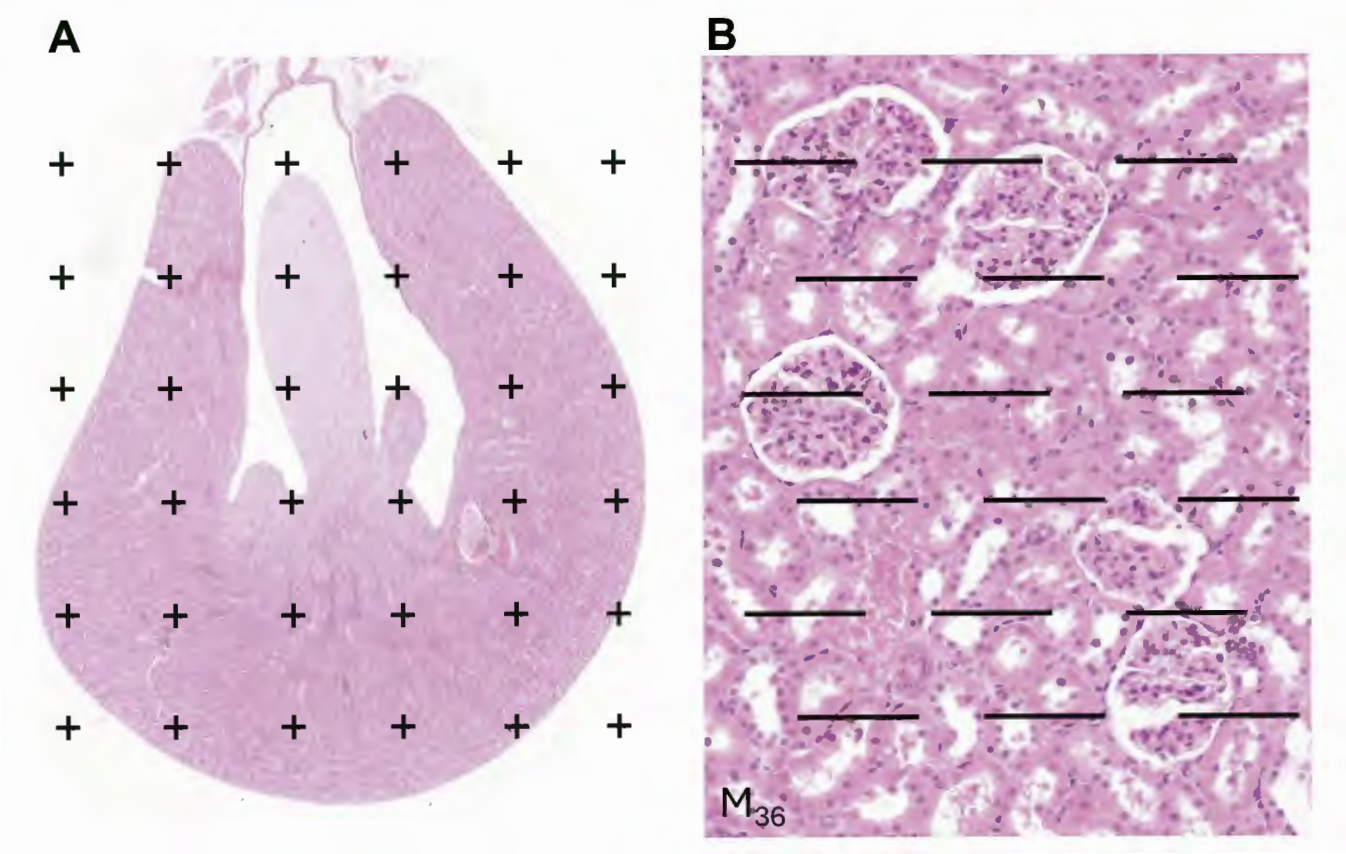
A
B
M_{36}

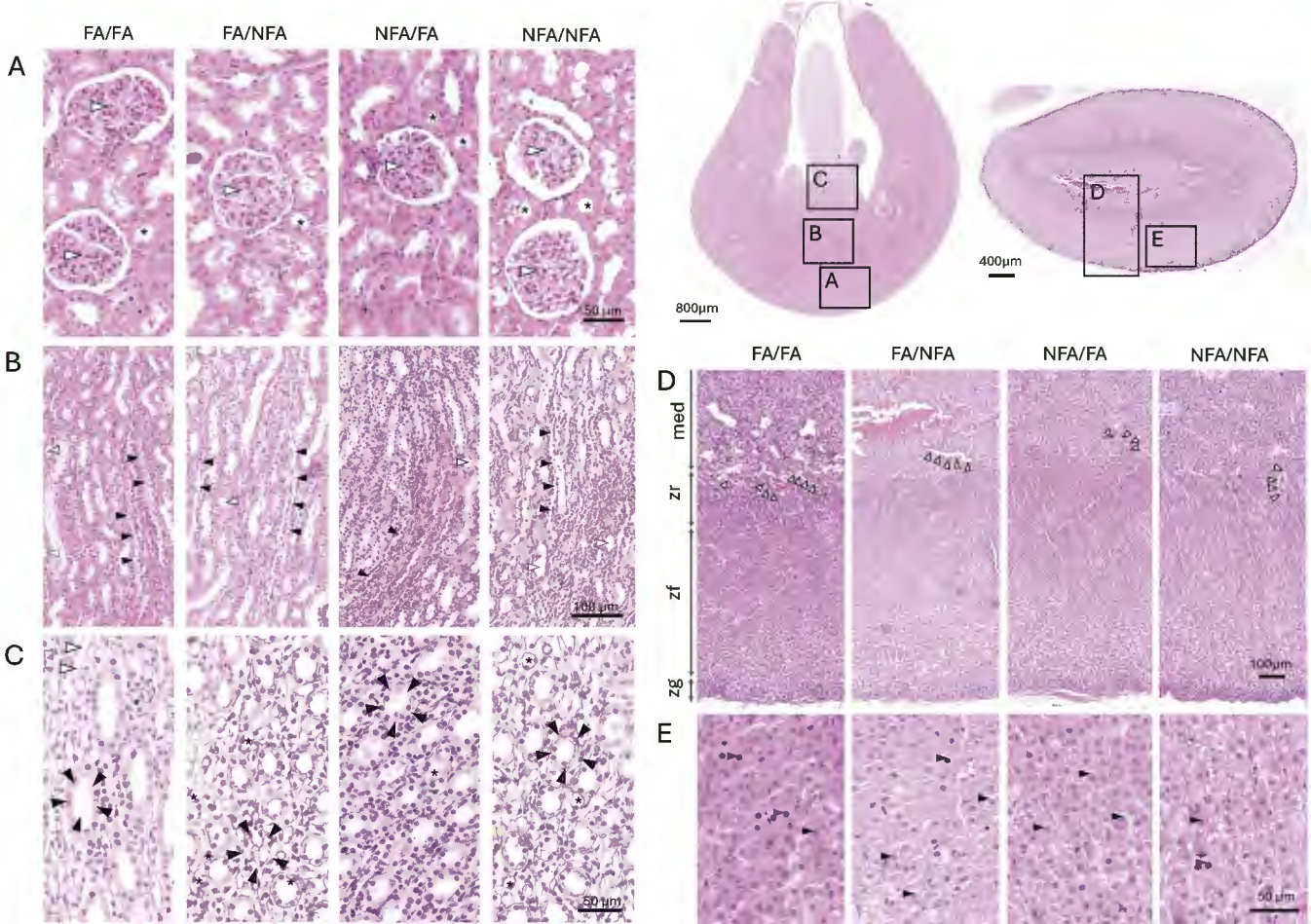
FA/FA
FA/NFA
NFA/FA
NFA/NFA
A
B
C
50 µm
100 µm
50 µm
C
B
A
800µm
D
E
400µm
FA/FA
FA/NFA
NFA/FA
NFA/NFA
D
med
zr
zf
zg
100µm
E
50 µm